Supporting Information

Engineering polymorphs in colloidal metal dichalcogenides: Precursor mediated phase control, molecular insights into crystallisation kinetics and promising electrochemical activity disulphides

Nilotpal Kapuria,[1a] Niraj Nitish Patil,[1a] Abinaya Sankaran,[a] Fathima Laffir,[a] Hugh Geaney,[a] Edmond Magner,[a] Micheál D. Scanlon,[a] Kevin M. Ryan[a] and Shalini Singh*[a]

[a] Department of Chemical Sciences and Bernal Institute, University of Limerick, V94T9PX, Limerick, Ireland

Corresponding author:

*Email: Shalini.Singh@ul.ie

Table of content:

1.1 TEM analysis of the MoS_2 nanosheets in conditions R2 and R4.

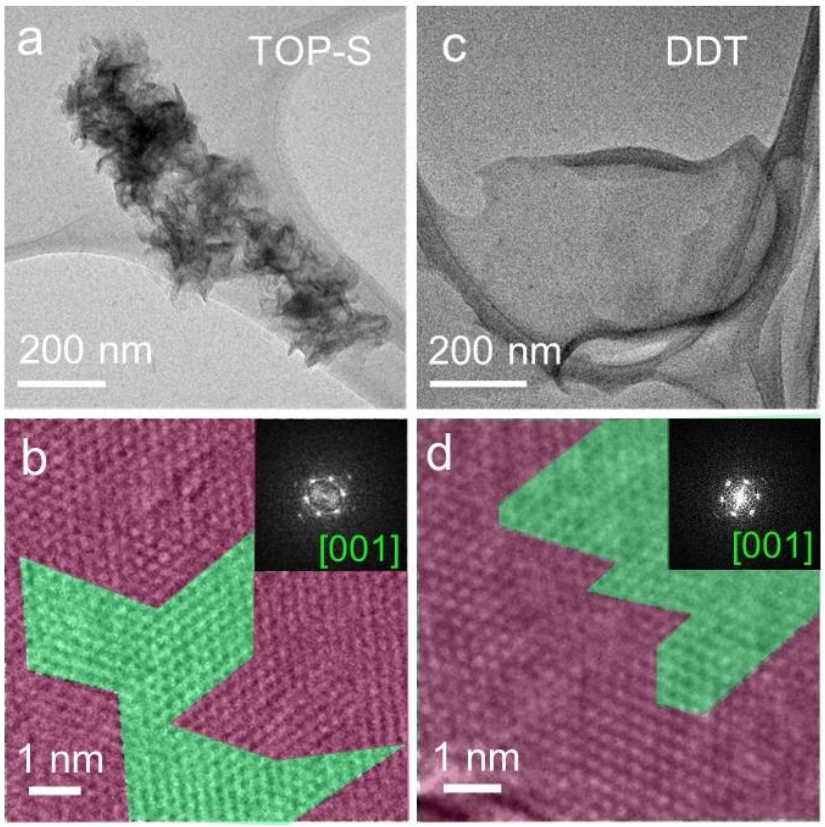

Figure S1 (a) Low magnification TEM image and (b)HRTEM of MoS_2 nanosheets prepared under condition R2; (c) Low magnification TEM image and (d)HRTEM of MoS_2 nanosheets prepared under condition R4. The green region shows 2H dominated area and magenta region exhibits 1T dominated areas of the nanosheets.

1.2.HRTEM of 1T phase of the MS_2 nanosheets.

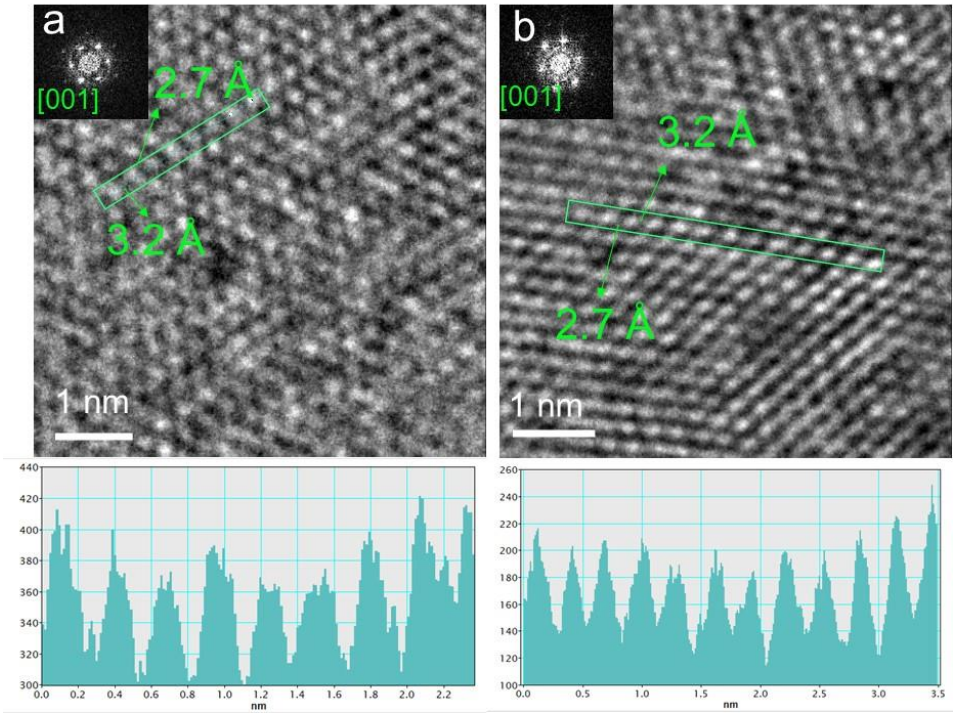

Figure S2. HRTEM of 1T phase of (a)MoS_2 and (b) WS_2 prepared in condition R6 and R6' with intensity profile displaying uneven M-M distance due to distorted atomic arrangement in the 1T phase.

1.3.UV-Vis-NIR absorption spectra of TMDs.

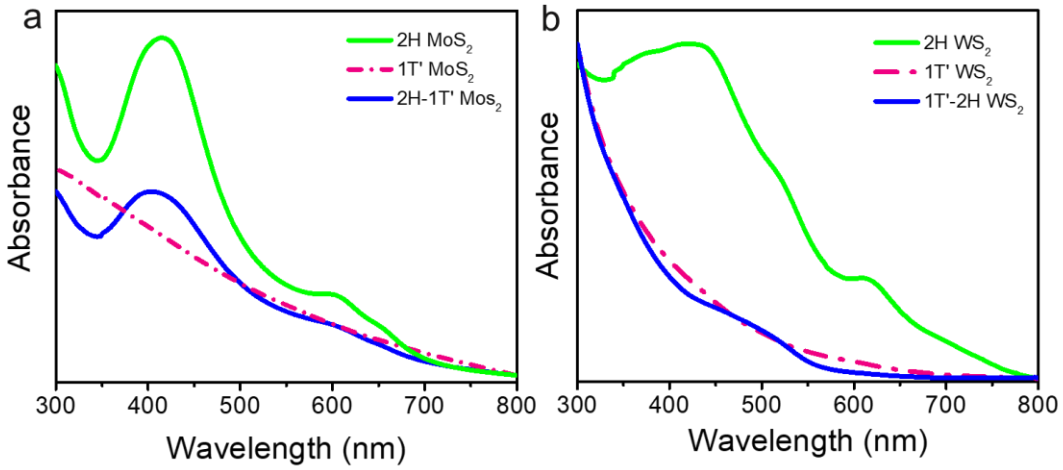

Figure S3. UV-Vis-NIR absorption spectra of the MoS_2 and WS_2 NCs synthesized.

1.4.Comparison of Mo and S-precurosors.

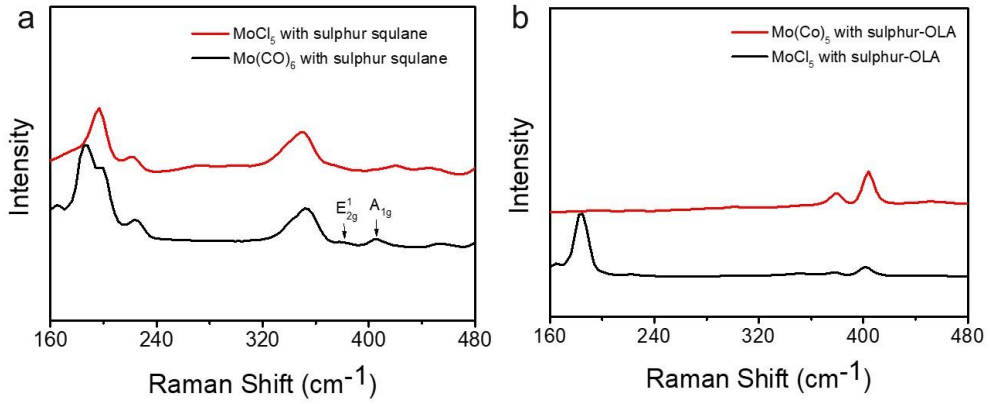

Figure S4. Mo-precursor reactivity comparison; Raman spectra of MoS_2 prepared with $MoCl_5$ and $Mo(CO)_6$ as metal source with (a) S-squalane and; (b) S-OLA. S-squalane suspension is reactive towards 1T phase formation, however lower reactivity of $Mo(CO)_5$ renders with some 2H phase formation. On the other hand, once OLA reduces S-precursor reactivity, 2H formation is increased. Even when highly reactive $MoCl_5$ is used, some 2H phase formation is noticed.

1.5.Reactivity comparison of W-precursors.

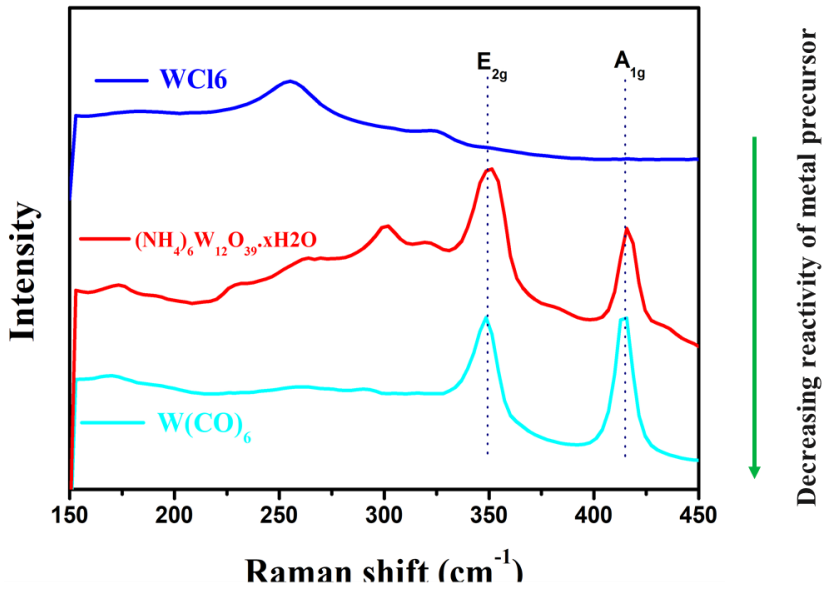

Figure S5. W-precursor reactivity comparison; Raman spectra of WS_2 prepared with WCl_6, $(NH_4)_6W_{12}O_{39}.xH_2O$ and $W(CO)_6$ as metal source with S-OLA. The reactivity trend of the W precursor is WCl_6> $(NH_4)_6W_{12}O_{39}.xH_2O$> $W(CO)_6$ towards 1T phase formation.

1.6. XPS analysis of the nanosheets synthesised using thiourea.

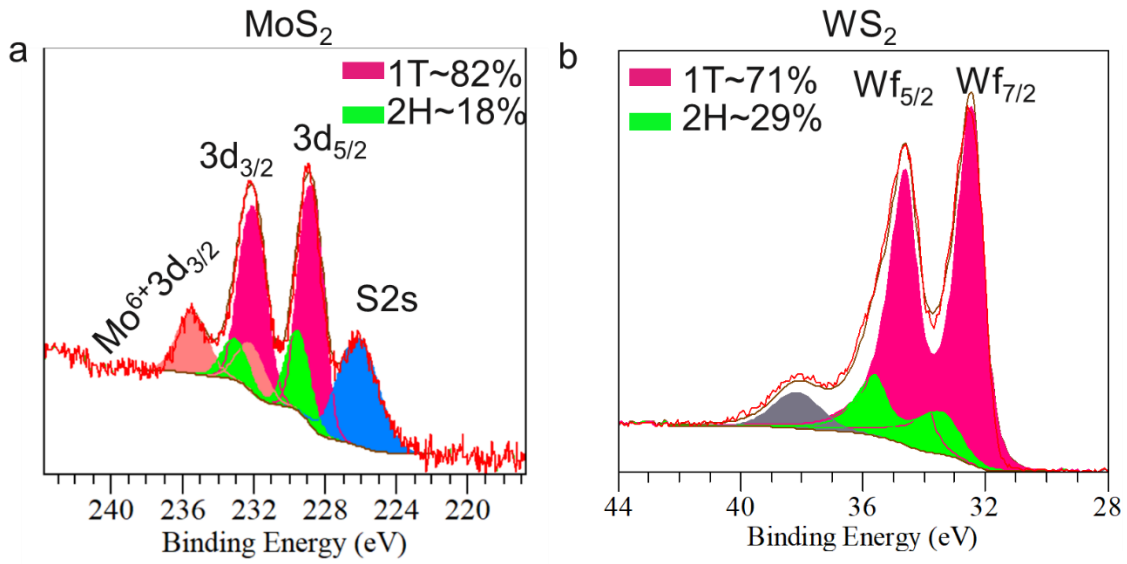

Figure S6. XPS analysis of as prepared (a) MoS_2 NCs, (b)WS_2 NCs synthesized using condition R6 and R6' respectively. Using thiourea leads to higher 1T phase formation due to the higher reactivity of thiourea. In the XPS spectra, the peaks at ~228 ($3d_{5/2}$) and ~232 eV ($3d_{3/2}$) correspond to 1T' phase, whereas the characteristic peaks of 2H MoS_2 phase appear at ~229 (Mo $3d_{5/2}$) and ~233 eV (Mo $3d_{3/2}$) while some MoO_3 formation is also visible as confirmed from the Mo^{6+} $3d_{3/2}$ peak at ~236 eV and 3d5/2 peak at ~232.5 eV. For 1T' WS2, the characteristic W4f peaks correspond to 31.5 ($W4f_{7/2}$) and 33.7 eV ($W4f_{5/2}$) where the grey peak corresponds to $W5P_{3/2}$ of WO_{3-x}.

1.7. ^{1}H NMR of S-oleylamine.

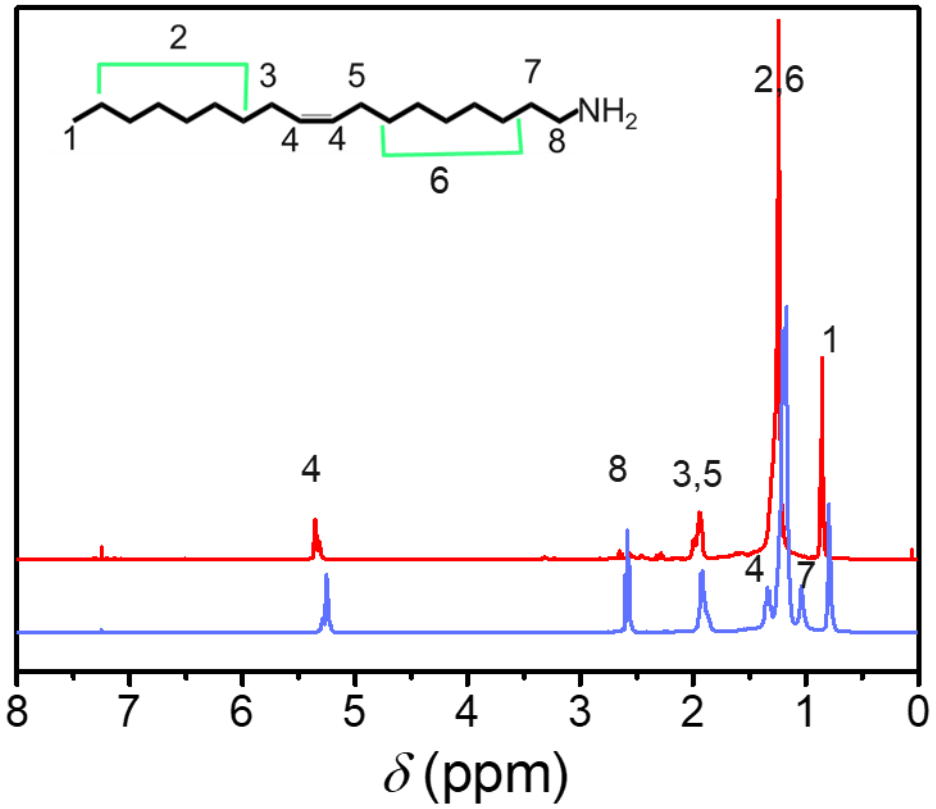

Figure S7. ^{1}H NMR of S-oleylamine solution (red spectra) heated at reaction condition. $CDCl_3$ used as reference displays peak ~7.26 ppm. The *a*-proton peak at ~2.7 ppm of the oleylamine (blue spectra) diminished after reacting with S.

1.8.Electrochemical performance.

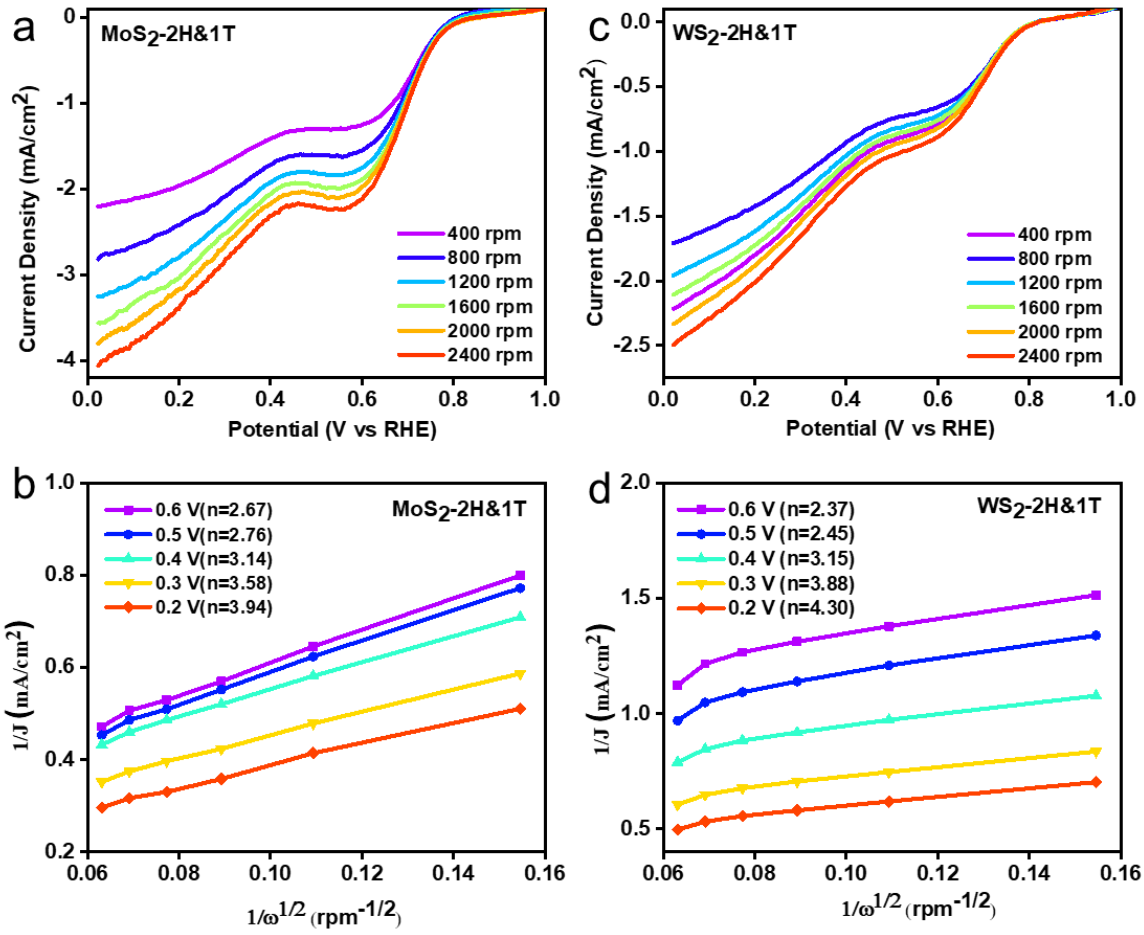

Figure S8. Rotating disc voltammograms of (a) Polytypic 2H-1T' MoS_2 at different rate of rotations in 0.1 M KOH, (b) Koutecky-Levich (K-L) plots of the current response of (b) 2H-1T' MoS_2 nanosheets;(c) Rotating disc voltammograms of 2H-1T' WS_2 nanosheets, (d) Koutecky-Levich (K-L) plots of the current response of 2H-1T' WS_2 nanosheets.

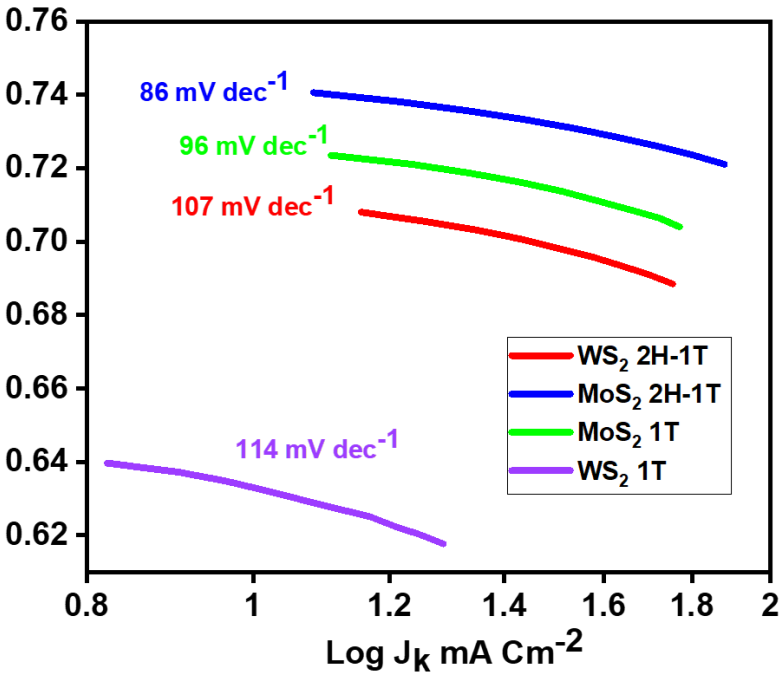

Figure S9. Tafel slope of the MoS_2 and WS_2 NCs. The MoS_2 polytypic material exhibits a low Tafel slope value of 86 mV/dec. compared to 1T' MoS_2 with 96 mV/ dec. A similar trend was followed in WS_2, where the polytypic WS_2 phase displays a Tafel slope of 107 mV/dec compared to the 1T' phase with 114 mV/dec. The polytypic electrocatalysts exhibit lower overpotential compared to 1T' counterparts attributed to improved ORR kinetics and lower corrosion rate.

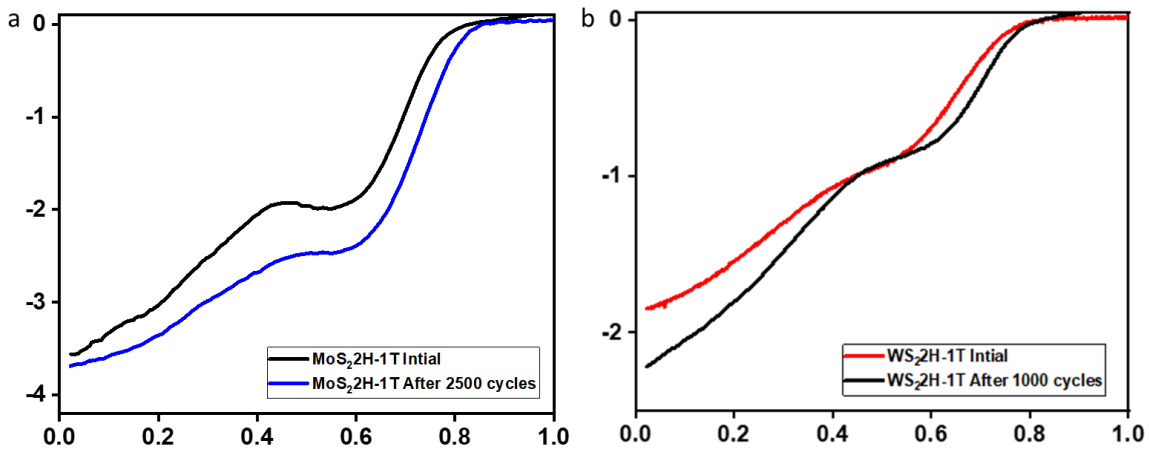

Figure S10. ORR stability test of the polytypic TMDs. The LSV was recorded at 1600 rpm after 2500 CV cycles for the MoS_2 sample and 1000 cycles for the WS_2 catalyst. We notice from the LSV that the MoS_2 electrocatalyst shows a positive shift in the onset potential from 0.82 to 0.84 V and a 32 mV positive shift in the half-wave potential with increased current density -3.68 $mA.cm^{-2}$ after 2500 CV cycles. This can occur due to ligand stripping, which is insulating in nature. In the case of WS_2, we observe a negative shift in the onset potential from 0.79 v to 0.78V and a 20 mV negative shift in half-wave potential with a lower current density of -1.8. $mA.cm^{-2}$. This is due to the catalyst's structural degradation, as seen in the TEM image shown in Figure S12.

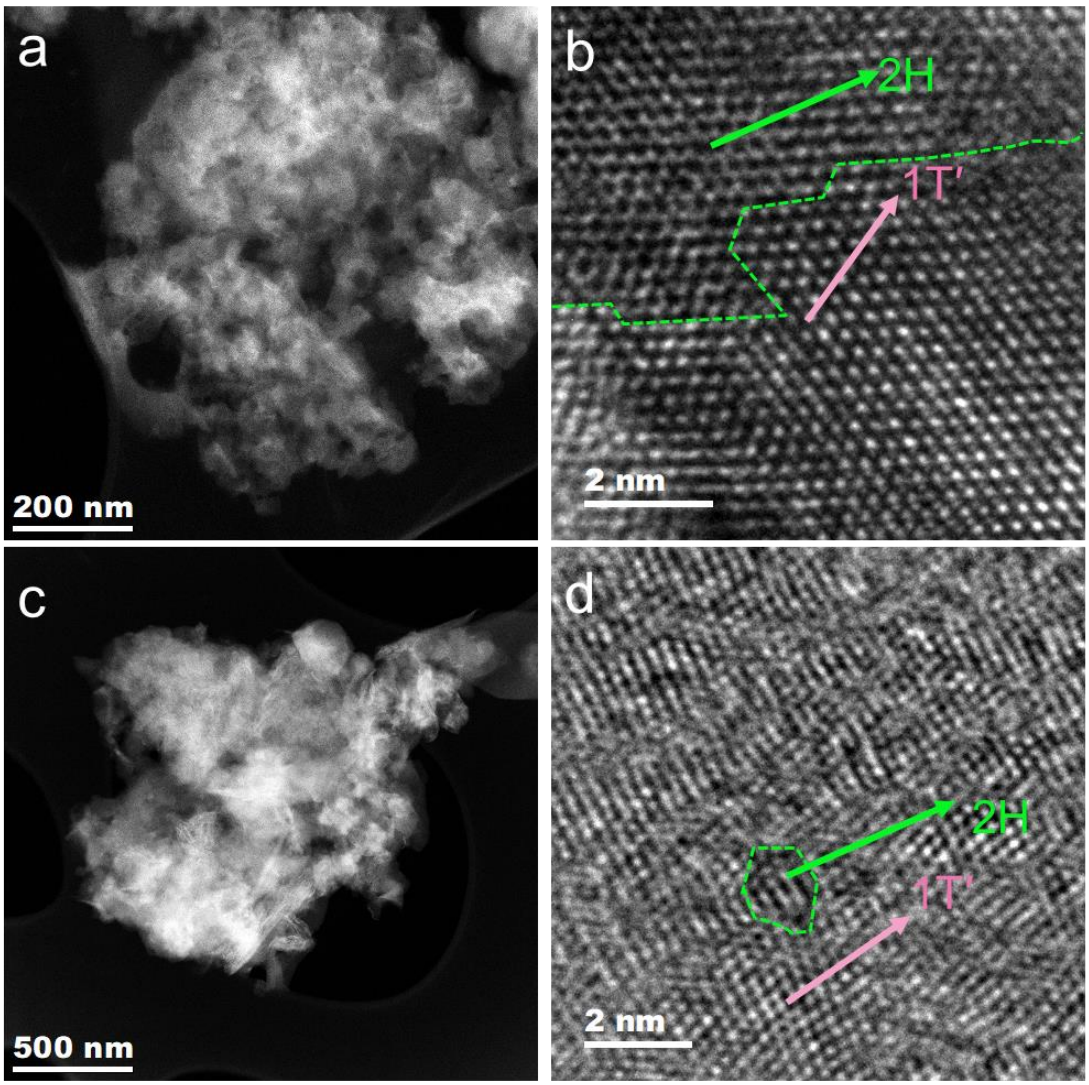

Figure S11. (a) STEM and (b) HRTEM image of polytypic MoS_2 nanosheets and (c) STEM and (d) HRTEM image of WS_2 after 1500 cycles of ORR. After 2500 cycles for MoS_2 and 1000 cycles for WS_2, the polytypic nature is still present.

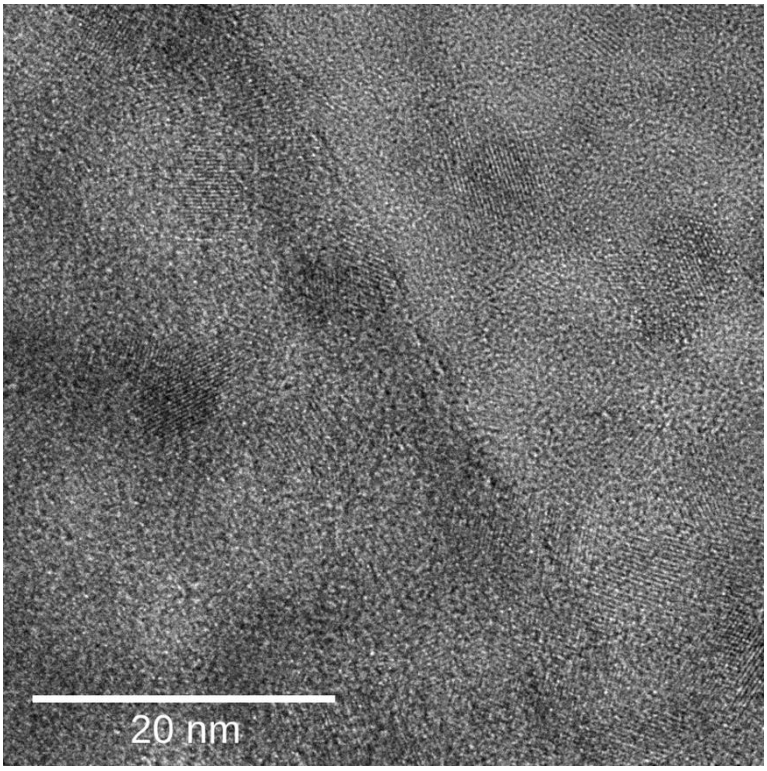

Figure S12. Degradation patches in the WS_2 nanostructure were observed after 1000 cycles.

Table S1 ORR data comparison of different phases of MS_2

Material	2H phase %	1T′ phase %	S-source	Onset potential (V vs. RHE)
MoS_2	100	0	S-OLA	0.76
MoS_2	58	42	*tert*-butyl disulphide-OLA	0.77
MoS_2	40	60	1-DDT-OLA	0.82
MoS_2	0	100	S-squalane	0.79
WS_2	77	23	S-OLA	0.74
WS_2	65	35	*tert*-butyl disulphide-OLA	0.79
WS_2	48	52	1-DDT-OLA	0.76
WS_2	17	83	S-squalane	0.77

The mixed phase MoS_2 with 2H (40%)-1T (60%) synthesised using 1-DDT as S source exhibits the highest onset of 0.82 V compared to mixed phase MoS_2 with 2H (58%) -1T (42%) synthesized using *tert*-butyl disulphide as sulphur source with onset of 0.77 V. This could be attributed to increased electronic conductivity for presence of higher percentage of 1T' phase in the MoS_2 polytype synthesized using 1-DDT.[1] However, in case of WS_2 we see samples with high 2H percentage (WS_2 2H(65%) - 1T(35%)) synthesized using *tert*-butyl disulphide as sulphur source exhibits a positive ORR onset of 0.79 V compared to WS_2 (0.76 V) mixed phase (2H (48%)-1T (52%)) with higher 1T phase synthesized using 1-DDT as S source. The deviance in WS_2 could be due to the lower stability of 1T' phase, thus, a higher percentage of 2H phase is required for the stability of the polytype.[2] But increasing the 2H phase in WS_2 further as for S-OLA is possibly detrimental for electronic conductivity resulting in a negative shift in onset potential. Overall, the polytypic NCs perform better than the monophase NCs. This is probably due to the presence of heterointerfaces beneficial for improved charge transfer and stability. The onset values are calculated from the polytype LSVs for ORR shown in Figure S13.

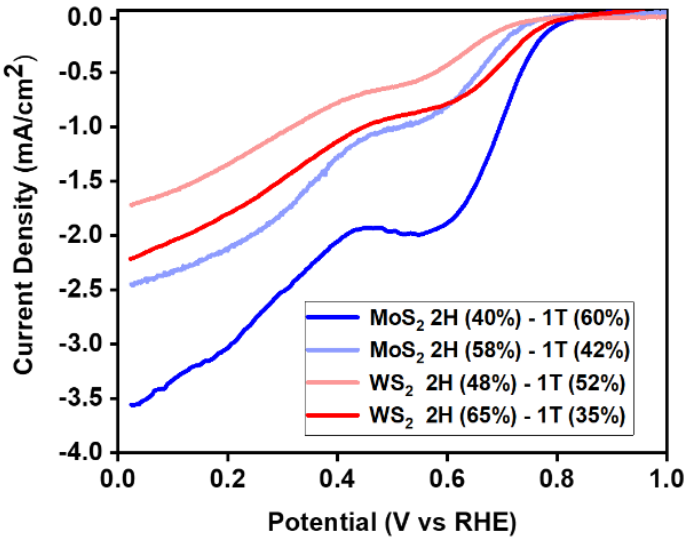

Figure S13. Comparison of LSVs of the polytypic MS_2 NCs.

Table S2. ORR comparison

Material	**Onset potential /V vs RHE**	**Synthesis Method**	**Reference**
MoS_2	0.78	Hydrothermal	Appl. Surf. Sci., 2020, 526, 146751
MoS_2	0.78	Solid-state synthesis	ACS Catal. 2016, 6, 5724–5734
WS_2	0.73	Solid-state synthesis	ACS Catal. 2016, 6, 5724–5734
MoS_2	0.76	Solid-state synthesis	ACS Appl. Mater. Interfaces 2020, 12, 20383
WS_2	0.76	Solid-state synthesis	ACS Appl. Mater. Interfaces 2020, 12, 20383
Polytypic MoS_2	0.82	Hot injection	**This work**
Polytypic WS_2	0.79	Hot injection	**This work**
1T MoS_2	0.90	Exfoliation	Nanoscale, 2018,10, 22549
2H MoS_2	0.79	Exfoliation	Nanoscale, 2018,10, 22549

References:

1. J. Q. Zhu, Z. C. Wang, H. J. Dai, Q. Q. Wang, R. Yang, H. Yu, M. Z. Liao, J. Zhang, W. Chen, Z. Wei, N. Li, L. J. Du, D. X. Shi, W. L. Wang, L. X. Zhang, Y. Jiang and G. Y. Zhang, *Nat Commun*, 2019, **10**.
2. Y. C. Lin, C. H. Yeh, H. C. Lin, M. D. Siao, Z. Liu, H. Nakajima, T. Okazaki, M. Y. Chou, K. Suenaga and P. W. Chiu, *Acs Nano*, 2018, **12**, 12080.